JOURNAL OF GEOPHYSICAL RESEARCH, VOL. 112, A07305, doi:10.1029/2007JA012313, 2007

Contrasting behavior of the thermosphere and ionosphere in response to the 28 October 2003 solar flare

Huixin Liu,[1] Hermann Lühr,[2] Shigeto Watanabe,[1] Wolfgang Köhler,[2] and C. Manoj[3]

Received 30 January 2007; revised 30 March 2007; accepted 16 April 2007; published 14 July 2007.

[1] We examined the thermospheric and ionospheric responses to the solar flare on 28 October 2003, utilizing simultaneous observations of the electron and neutral density from the CHAMP satellite. Rapid thermospheric response within a few minutes was observed. In addition, the neutral and plasma perturbations contrasted each other remarkably. First, their temporal development differed. Though started nearly simultaneously, the plasma perturbation developed much faster and to a larger amplitude than its neutral counterpart. Second, their latitudinal distributions differed. At the initial stage of the response, the neutral density was enhanced by 20% almost homogeneously at all latitudes below 50°N/S. In comparison, the plasma disturbance exhibited a distinctive latitudinal structure, with largest density enhancements of 68% at the dip equator, moderate increase of ~20% at midlatitudes, and depression up to 35% around 15°N/S. This suggests a decoupling between the neutral and plasma disturbances during this stage. The plasma-neutral coupling via ion drag was found to become important about 2–3 hours after the flare bursts. Another interesting feature is that the equatorial ionization anomaly was significantly weakened during the flare. The observations demonstrated that electrodynamics related to the equatorial fountain dominated the photochemistry in controlling the flare-induced plasma density disturbances on 28 October 2003. This differs considerably from the nearly linear cos(SZA) dependence of flare-induced total electron content enhancements.

Citation: Liu, H., H. Lühr, S. Watanabe, W. Köhler, and C. Manoj (2007), Contrasting behavior of the thermosphere and ionosphere in response to the 28 October 2003 solar flare, *J. Geophys. Res.*, *112*, A07305, doi:10.1029/2007JA012313.

1. Introduction

[2] Solar flare is one of the most extraordinary processes occurring on the Sun. It ejects enormous amounts of energy into the outer space in a very short time ranging from a few minutes to a few hours. The extreme ultraviolet (EUV) and X-ray emissions usually increase dramatically during solar flares. These enhanced emissions cause extra ionization of the neutral components in the Earth's upper atmosphere and hence immediate increases in the electron density over a wide altitude range from the ionospheric *D* region up to the *F* region [*Thome and Wagner*, 1971]. This consequently leads to various sudden ionospheric disturbances (SIDs) such as the sudden frequency deviation (SFD) [*Donnelly*, 1969; *Liu et al.*, 1996], the sudden phase anomaly (SPA) [*Ohshio*, 1971], the short wave fadeout (SWF) [*Stonehocker*, 1970], and the geomagnetic crochets [*Richmond and Venkateswaran*, 1971], etc. The ionospheric responses to solar flares have been examined since 1960s, and comprehensive reviews can be found in the work of *Mitra* [1974] and *Davies* [1990]. Recently, the use of the total electron content (TEC) from the global positioning system (GPS) network has greatly advanced SID studies. It is now generally accepted that the sudden increase of TEC (SITEC) has a roughly linear relation with the cosine of the solar zenith angle (SZA) [*Zhang and Xiao*, 2003, 2005] but with nonnegligible residuals due to the background atmospheric composition, particularly the ratio of $[N_2]/[O]$ [*Tsugawa et al.*, 2006].

[3] Most studies reporting terrestrial effects of solar flares have so far focused on the ionospheric aspects of the effects, while mentioned little about the thermosphere. The thermosphere, with its large mass and high heat capacity, is generally expected to be sluggish in responding to transient events like solar flares, which typically lasts less than 1 hour. However, in the upper thermosphere where the air density is relatively low, early disturbances could be detected by instruments with high sensitivity. This has been recently demonstrated by several studies using the high-accuracy accelerometer on board the CHAMP satellite [*Liu and Lühr*, 2005; *Bruinsma et al.*, 2006]. These studies showed that the thermosphere reaction during magnetic storms could be

[1] Earth and Planetary Science Division, Hokkaido University, Sapporo, Japan.
[2] GeoForschungZentrum Potsdam, Potsdam, Germany.
[3] Magnetotellurics Division, National Geophysical Research Institute, Hyderabad, India.

0148-0227/07/2007JA012313$09.00

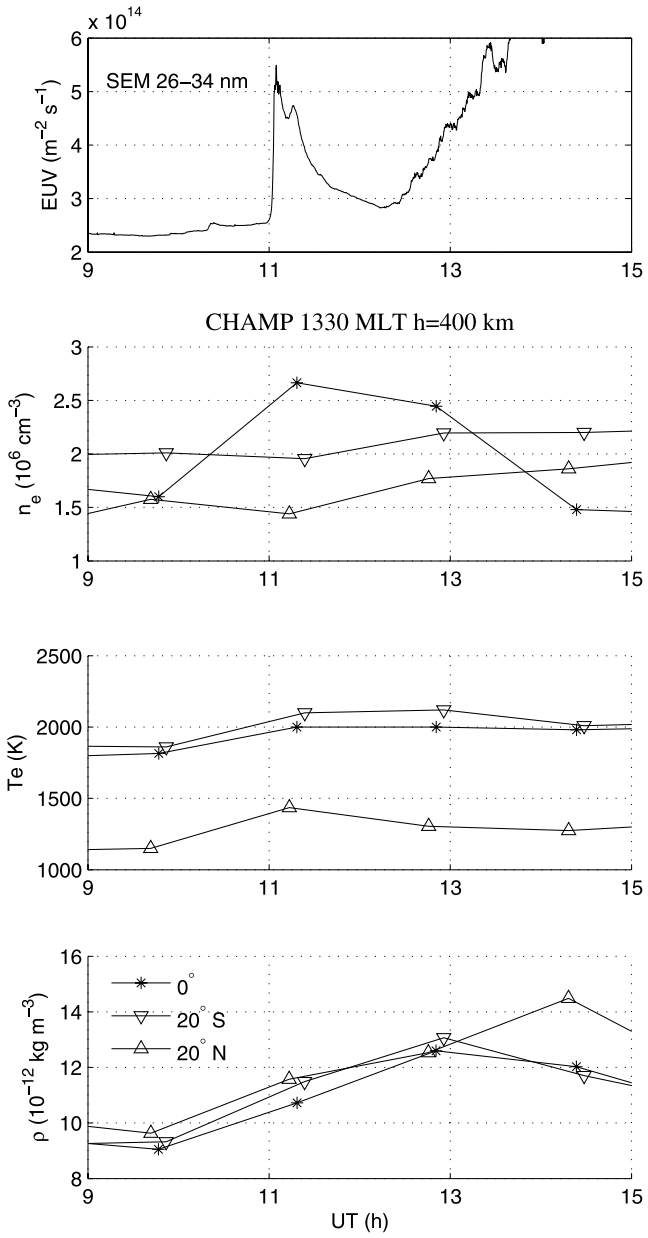

Figure 1. The time variation of the solar EUV flux observed by SOHO SEM on 28 October 2003, along with noontime equatorial electron density (n_e) and temperature (Te) and neutral mass density (ρ) measured by CHAMP at three dip latitudes (0° and 20°N/S). Note though started almost simultaneously, n_e perturbation developed much faster and to a larger amplitude than its thermospheric counterpart. The recovery time of ρ was a few hours longer than n_e, as expected.

much faster than traditionally expected. *Liu and Lühr* [2005] have also pointed out the rapid and unmistakable response of the thermospheric density to the impulsive event of a storm sudden commencement within 30 min. In addition to directly responding to the enhanced UV/EUV heating during solar flares, the thermosphere may also indirectly respond to it via the enhanced thermosphere-ionosphere (T-I) coupling induced by increased electron density and ion drag. This speculation forms the primary motivation for our study presented here. To serve this purpose, the polar orbiting satellite CHAMP is employed, which provides simultaneous measurements of the thermospheric density, the electron density, and temperature in both hemispheres. Details about the CHAMP satellite and related data processing can be found in the work of *Liu et al.* [2005]. In the following, we focus on the solar flare effect on 28 October 2003, when the CHAMP satellite was in the 1330–0130 LT meridional plane. The TEC response to this solar flare has been studied by *Zhang and Xiao* [2005], *Tsurutani et al.* [2005, 2006], and *Liu et al.* [2006], and the thermospheric density response has been shown by *Sutton et al.* [2006]. In our study, we focus on the large-scale structure of the flare-induced disturbances and in particular on the coupling between the thermosphere and ionosphere in the equatorial anomaly regions during such a transient event.

2. Observations

[4] In this section we present three sets of observations to demonstrate some major terrestrial effects of the solar flare. They include the ionospheric and thermospheric density from CHAMP, and magnetometer measurements from ground stations. Dip latitudes are used in the presentation below unless otherwise noted.

2.1. Temporal Variation at Equatorial and Low Latitudes

[5] The 28 October 2003 solar flare was a large X-17 class event, with a prominent peak around 1110 UT in the X rays, and ended at 1124 UT. Since the solar radiation in the EUV wavelength range is more directly related to the *E* and *F* region ionosphere, we present in Figure 1 the EUV (26–34 nm) measurement from the SOHO SEM instrument as an indicator for the general development of the flare. The EUV during the flare peaked first at 1105 UT and then at 1116 UT with a smaller magnitude. The subsequent panels in Figure 1 show the corresponding time history of the electron density (n_e) and temperature (Te), and thermospheric mass density (ρ) observed by CHAMP near 1330 magnetic local time (MLT) at three dip latitudes, 20°N (upward triangle lines), 0° (star lines), and 20°S (downward triangle lines). The measurements were all adjusted to a common altitude of 400 km to eliminate altitude-induced variations. Since CHAMP flew from north to south during these dayside tracks on 28 October 2003, covering ~20° in latitudes every 5 min, a 5-min time shift applies between these three adjacent locations. The poor resolution (93 min) seen here is intrinsic for many satellites measurements, due to the fact that it takes at least one orbit period for the satellite to revisit the same latitude and local time.

[6] In response to the prominent flare EUV peaks, both the ionospheric and thermospheric quantities underwent strong disturbances as shown in Figure 1. At the dip equator (star lines), the largest n_e enhancement of about 68% was observed at 1118 UT. This enhancement lasted for 1.5–3 hours (1.5 hours time ambiguity is due to the orbit period) before it recovered to preflare level. In spite of the fact that 20°S located at lower solar zenith angle (SZA) than the dip equator (refer to bottom panel of Figure 2), the

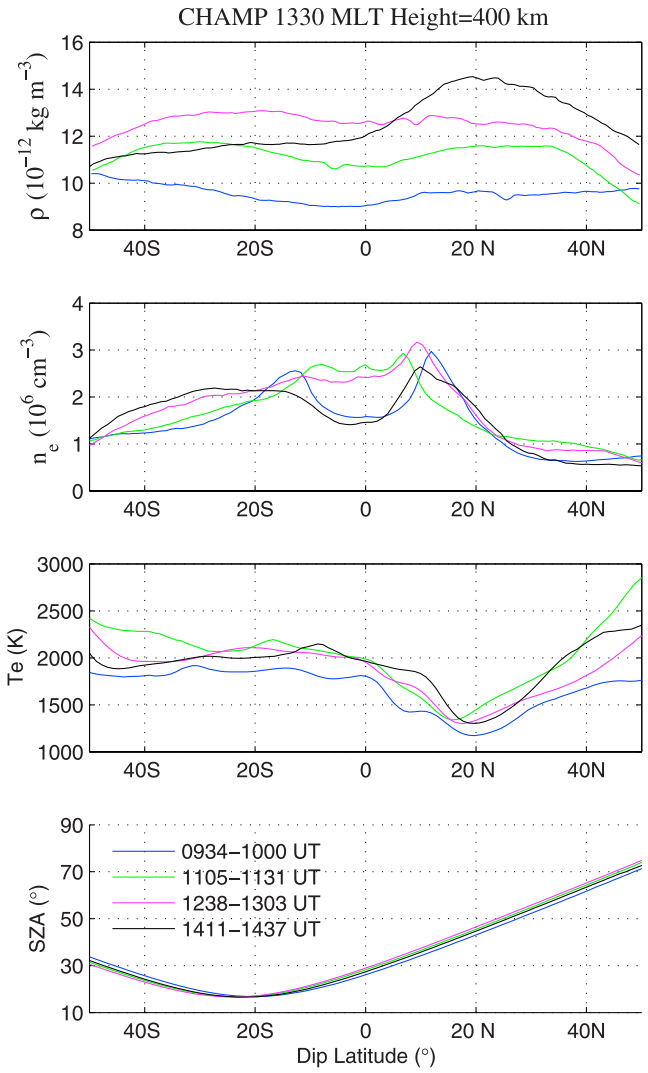

Figure 2. The thermospheric mass density, electron density and electron temperature observed by CHAMP during four consecutive satellite tracks on 28 October 2003, along with the solar zenith angle. CHAMP flew from north to south and the crossing times at 50°N and 50°S for each track are labeled in the bottom panel. Attention is drawn to the strong weakening of the EIA structure immediately after the flare peaks and the large neutral density bulge in the northern hemisphere ~3 hours after the flare peaks.

electron density here enhanced by only ~12% (near 1300 UT) even 1.5 hours after the EUV bursts. In the northern hemisphere at 20°N, a n_e decrease was first recorded at 1113 UT before a 22% enhancement was observed at ~1245 UT. Therefore responses of n_e to this solar flare at the above three locations differ not only in magnitudes but also in temporal variations. It is faster and stronger at the dip equator than at other latitudes, regardless of the SZA. The response at 20°S and 20°N started later and reached smaller maxima but lasted longer. The electron temperature experienced rather small disturbances, with enhancements of about 10% at the dip equator, 12% at 20°S, and 25% at 20°N. The time variations of Te are similar at these three locations.

[7] In comparison to the ionospheric disturbances, several features stand out from the thermospheric responses. First, thermospheric density enhancements at the three locations were observed almost simultaneously after the flare EUV bursts, with an almost equal growth rate as indicated by the nearly identical slopes between 1000 and 1300 UT. Second, the growth of ρ at 20°S and at the dip equator continued till at least 1300 UT (1.5 hours after the flare), where it reached a maximum of about 40%. However, at 20°N, the growth of ρ lasted 1.5 hours longer before reaching a maximum with 50% enhancement. Third, at the equator, ρ attained its maximum value about 1.5 hours after n_e reached its maximum. In addition, the recovery of ρ was slower than that of n_e as well. It was still about 20% higher than preflare level even 4.5 hours after the flare, while n_e already decreased to the preflare level after 3 hours.

2.2. Latitudinal Structures

[8] Figure 2 presents in detail the latitudinal structures of noon-time n_e, T_e, and ρ simultaneously observed by CHAMP during four consecutive satellite tracks between 50°S–50°N. The latitudinal resolution is 0.7° for ρ and 1° for n_e and T_e. As the solar zenith angle is an important controlling factor of the photoionization, it is plotted in the bottom panel for corresponding satellite tracks. The fact that the SZA curves fall almost on top of each other indicates that the four tracks are well repeating each other in latitudes and local times (owing to the polar orbit and its slow precessing rate). The starting time at 50°N and ending time at 50°S are labeled for each track in the bottom panel. Among the four tracks, the blue one was before the EUV bursts. The green one covered the two EUV bursts at 1105 UT and 1116 UT (corresponding to CHAMP's position at 50°N and 10°N in the green lines). The pink and black ones are respectively tracks ~1.5 hours and 3 hours after the flare ended.

[9] First, we examine the green curves. CHAMP passed from 50°N to 10°N within 10 min after the flare, where about 20% enhancement in ρ had already developed at latitudes below 40°N. This demonstrates the rapid response of the thermosphere to the solar flare within a few minutes. Though a second EUV burst of smaller magnitude occurred when CHAMP was crossing 10°N at 1116 UT, the ρ enhancement at latitudes between 40°S and 10°N is of similar magnitude to that observed earlier at northern midlatitudes. In addition to the elevated density, it is also evident that the equatorial mass density anomaly [*Liu et al.*, 2005, 2007] grew more pronounced compared to the preflare curve, with two prominent density crests at middle latitudes.

[10] Contrasting to the almost homogeneous ρ enhancement at all latitudes within 40°S–40°N, the n_e perturbation exhibited a complicated latitudinal structure. Strong enhancements reaching 68% were observed within 10° from the dip equator as shown by the green curve. Enhancements of 20% can also be recognized at middle latitudes between 20°–40°N/S. However, in regions where the EIA crests are usually located (about 15°N/S), the electron density decreased by up to 35% instead of increasing. The lack of enhancement of n_e shortly after the flare at 1105 UT shown in Figure 1 at 20°N and 20°S actually reflects this latitudinal structure. Compared to the typical EIA structure shown in the preflare curve, it is

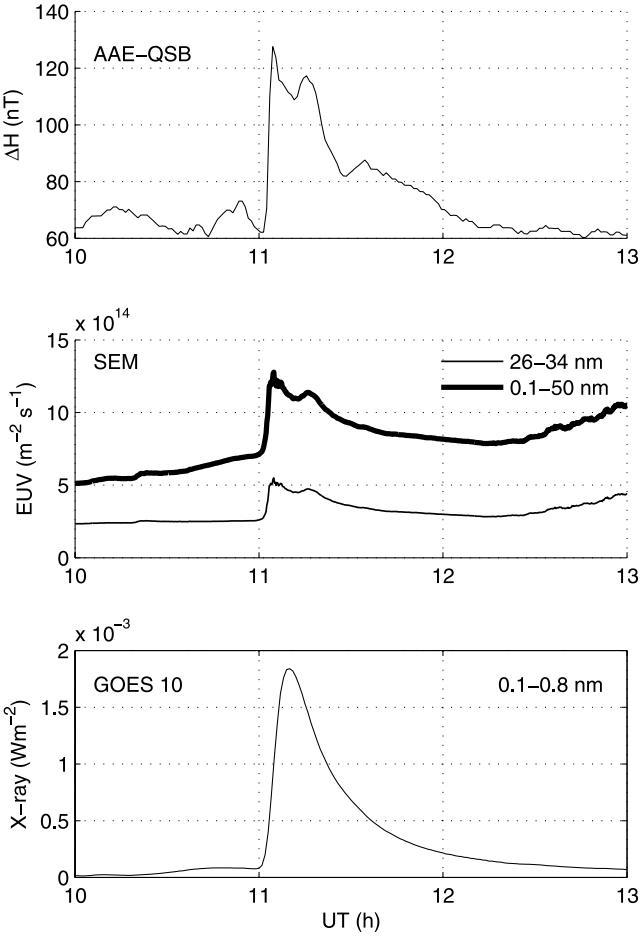

Figure 3. The EEJ index at an equatorial station Addis Abeba (AAE, 9°N 39°E geographic, LT = UT + 2.6 hours) during a period covering the solar flare on 28 October 2003 and the corresponding EUV and X ray observed by SOHO SEM and GOES 10, respectively. This EEJ index represents the EEJ current strength (see text for details). Note the EUV's double-peak variation is closely reflected in the EEJ development during the flare.

unmistakable that the EIA structure was significantly weakened. The trough region was filled up with almost twice as much electrons as the preflare ones. At the same time, two EIA crests moved closer to each other by about 10° in latitudes.

[11] Examining subsequent satellite tracks reveals not only consistent temporal variations described in Figure 1 and related section but also the development of the whole large-scale latitudinal structures. About 1.5 hours after the flare, the thermospheric density was observed to grow yet another 20% as shown in the top panel, with similar amplitudes at low and middle latitudes. The growth was found to have terminated in the southern hemisphere and at the dip equator about 3 hours after the flare, as depicted by the black curve. At latitudes poleward of ~10°N, however, ρ continued to rise and reached an enhancement of ~50% at 1418 UT. This resulted in a strong hemispheric asymmetry, with ρ being about 25% higher at 20°N than that at 20°S.

[12] The n_e curves in the second panel demonstrate the great variations of EIA before and after the solar flare. The EIA structure was rather normal before the flare (blue curve), with a slightly higher northern shoulder, likely due to combined effect of higher $[O]/[N_2]$ in the northern hemisphere at this time of the year [*Tsugawa et al.*, 2006] and the northward transequatorial wind. However, the EIA structure changed considerably shortly after the flare (green curve), with almost 100% enhancement of the electron density at the dip equator and equatorward shifting of the EIA crests by ~5°. This weakening or reconfiguration of the EIA persisted to the subsequent satellite track, where a stronger hemispheric asymmetry also formed. The EIA northern crest centered at 10°N was about 45% higher than the southern crest. This high-density crest developed one orbit (1.5 hours) earlier than the neutral density bulge near 20°N, hence suggesting a possible cause-effect relation as we will discuss later. The EIA was observed to have recovered to its usual shape ~3 hours after the flare.

[13] The electron temperature showed a rather small increase about 10% (200–300 K) after the flare. Though a rough anticorrelation is usually expected between the electron density and temperature above the F region peak, T_e did not show complicated latitudinal structures as the electron density. The trough at about 20°N was observed before and after the flare and therefore seems to be a feature which has nothing to do with the solar fare. This feature is reflected in the fourth panel of Figure 1, where the curve for 20°N departed significantly from the other two.

2.3. Responses of the Equatorial Electrojet

[14] Solar flare effects on the equatorial electrojet (EEJ) and related mechanisms have been studied in great details before [e.g., *Rastogi et al.*, 1999; *Manju and Viswanathan*, 2005, and references therein]. Our examination of the EEJ response to the 28 October 2003 flare in this section is intended to illustrate the flare effect on the E region ionosphere, not to critically evaluate the underlying processes of the EEJ.

[15] The top panel in Figure 3 displays an EEJ index at an equatorial station Addis Abeba (AAE, 9°N 39°E geographic) during a period covering the solar flare. This EEJ index represents the EEJ current strength [*Manju and Viswanathan*, 2005] and was computed by subtracting the daily variation of the ΔH component observed at a midlatitude station, Qsaybeh (QSB, 34°N 36°E geographic), from the ΔH recordings at AAE, which is 1° north of the geomagnetic dip equator. Further details about the calculation of the EEJ index can be found in the work of *Manoj et al.* [2006]. Measurements of EUV from SOHO SEM and X rays from GOES 10 are displayed in Figure 3 for the corresponding period. The diurnal variation of the EEJ index at AAE typically consists of a rapid growing phase in the morning, a maximum at local noon (0900 UT), and a gradual declining phase afterwards. When the EUV peaked around 1105 UT and 1116 UT on 28 October 2003, AAE was passing 1340 LT and 1350 LT, and hence should be in the declining phase. However, doubling of the EEJ intensity was observed immediately after the flare explosions. In particular, these dramatic enhancements followed neatly the EUV's double-peak intensification. The close relation between the ΔH component and the EUV bursts demonstrates

the solar flare effects in the *E* region. As the electric field in the EEJ region has been shown to decrease during flares [*Manju and Viswanathan*, 2005], the doubling of the EEJ intensity may suggest large increases of the *E* layer electron density over 100%.

3. Discussion

[16] The solar flare effects on the coupled thermosphere and ionosphere on 28 October 2003 were investigated utilizing simultaneous observations around 1330 MLT from the CHAMP satellite. Rapid responses within a few minutes after the flare EUV peaks were recorded in both the thermospheric and ionospheric densities at low and middle latitudes. This observed thermospheric response time is over 10 times faster than the time constant for neutrals to respond to a change in the ion drag, which was simulated and observed to be 1 hour or more [e.g., *Killeen and Roble*, 1984; *Conde et al.*, 2001]. In addition to this fast thermospheric response, the contrasting behaviors between the neutral and ionized part of the upper atmosphere, and the significant reconfiguration/weakening of the EIA are particularly interesting aspects of the solar flare effect.

[17] First, the flare-induced thermospheric and ionospheric disturbances differ in their temporal development. Although both the electron and thermospheric density at the dip equator started to grow within 10 min after the flare, their growth rates are different. A 68% enhancement was soon reached at ~1118 UT in the electron density, but only 20% enhancement was observed in the thermospheric density. This yields a n_e growth rate over three folds of that in ρ in the initial phase of the response. The equatorial electron density growth terminated within 93 min after the flare, while the thermospheric density continued to grow for another 1.5 hours before attaining its maximum enhancement of 40%. The electron density was found to recover to the preflare level about 3 hours after the flare, in contrast to a ~20% enhancement in the thermospheric density lasting to even 4.5 hours after the flare. Therefore though started almost simultaneously, the ionospheric perturbation developed much faster and to a larger amplitude than its thermospheric counterpart. The recovery time of the thermosphere was a few hours longer than the ionospheric one, as expected.

[18] Second, the latitudinal distribution in the flare-induced neutral and plasma perturbations contrasts each other remarkably. In the initial phase of the response (within 20 min after the flare bursts), the neutral density was enhanced almost homogeneously at all latitudes below about 50°N/S. In comparison, the plasma density disturbance exhibited a distinctive latitudinal structure. It consisted of largest enhancements at the dip equator, moderate increases at midlatitudes, and considerable depletions around 15°N/S. Therefore the neutral and plasma perturbations seemed to be decoupled during this stage. However, the situation changed significantly about 1.5 hours after the flare bursts. CHAMP observed a high density bulge first in the plasma centered near ~10°N at 1248 UT and then in the neutrals centered near ~20°N at 1418 UT. This led to similar latitudinal asymmetries in the plasma and neutral densities but with a ~1.5 hours time shift. The neutral density bulge is possibly a consequence of the plasma crest as explained below. The building up of the plasma in the northern EIA crest can give rise to higher ion drag and enhanced chemical heating released from charge-exchange process in the *E* region. This would slow down the day-to-night transport of the energy and mass and lead to atmospheric expansion over the heating region as well. These processes consequently cause the neutral density in the north to grow higher but with a time lag (within ~1.5 hours) and a latitudinal offset (see details in the work of *Liu et al.* [2005, 2007]). The time lag is consistent with the time constant (1 hour or more) for neutrals to respond to a momentum forcing [e.g., *Killeen and Roble*, 1984; *Conde et al.*, 2001]. In summary, these features suggest that in the initial phase of the flare response, the neutral and plasma disturbances are likely decoupled from each other. After the explosive effect subsidies (~2–3 hours), however, the plasma-neutral coupling via ion drag sets in to play an important role in controlling the neutral processes and hence resulting in similar neutral and plasma disturbances.

[19] Another prominent feature of the flare effect is the significant weakening of the noontime EIA structure. This was demonstrated by the variation of the n_e profiles displayed in Figure 2. The n_e exhibited a typical EIA structure before the flare. Shortly after the flare burst, however, the latitudinal profile changed dramatically. We observed an almost complete filling up of the EIA trough and a 5° equatorward movement of both EIA crests. What might have caused this change? Although the photoionization is enhanced during the flare, the solar zenith angle plays little role at 400 km altitudes. This is because the atmosphere at such altitude is optically thin and the solar radiation intensity is nearly independent of the SZA at low latitudes. The EIA is known to have a strong longitudinal dependence in the Atlantic region (−90°–0° geog. longitude). However, being at ~50° geog. longitude in the preflare pass and at 26° geog. longitude following the flare, the longitudinal effect well outside the Atlantic region is relatively small and unlikely to make up the large changes observed. Further processes therefore must be in operation. Also, this is likely to be the electrodynamics related to the equatorial fountain. The weakening of the EIA indicates a weakening of the equatorial fountain. It would slow down the upward drift of the plasma and its subsequent field-aligned diffusion. This consequently results in a reconfiguration of the EIA structure, with relatively higher electron density at the dip equator and shorter distance between two EIA crests as observed.

[20] It is not very clear what might have led to the weakening of the equatorial fountain. One possibility is a drop in the eastward electric field, which is the direct driver of the fountain. We know that the daytime electric field is directly produced by the lower thermospheric tidal winds via *E* region dynamo process [see, e.g., *Kelley* 1989, section 3.3]. A variation in the electric field could be induced by significant changes either in the global-scale wind or in the conductivity distribution on the dayside. Among these two, changes in the conductivity distribution (especially in the vertical direction) are more likely and rapidly during solar flares. As pointed out, for instance, by *Richmond and Venkateswaran* [1971] and *Richmond* [1973], the ratio of the Hall and Pedersen conductance is a critical factor in regulating the dayside dynamo. It is known that

great solar flares have strongest effect in the *D* region [*Mitra*, 1974]. Thus the (particularly Hall) conductivity below 100 km can greatly increase due to extra ionization by the X rays. This can significantly change the Hall/Pedersen conductance ratio as demonstrated by *Manju and Viswanathan* [2005] and hence modulate the dynamo electric field. Furthermore, this new conducting layer may also briefly enable neutral winds below 100 km to come into play in driving the dynamo system. Since the large-scale wind system in the vicinity of the dynamo region is highly height-dependent [e.g., *Greenfield and Venkateswaran*, 1968], the resulting dynamo electric field can consequently be altered at a similar timescale as that of the conductivity perturbations (which closely follow the solar flare).

[21] Therefore the flare-induced *F* region electron density disturbances observed by CHAMP in equatorial and low latitudes should be a combined effect of the photochemistry and the electrodynamics related to the equatorial fountain. The latter has been observed to dominate the former during the 28 October 2003 flare. This differs remarkably from the nearly linear cos(SZA) dependence of flare-induced TEC enhancements [*Zhang and Xiao*, 2003, 2005], which is the integrated effect over all ionospheric layers.

[22] Finally, since the terrestrial effect of solar flares depend evidently on the detailed spectrum of the radiation and also the flare locations on the solar disc [*Donnelly*, 1976; *Afraimovich et al.*, 2002; *Tsurutani et al.*, 2005; *Liu et al.*, 2006], it is highly possible that the thermospheric and ionospheric responses would vary from flare to flare.

[23] **Acknowledgments.** We thank A. Richmond, H. Fujiwara and A. Saito for helpful discussions and D. Cooke for processing the CHAMP PLP data. Institutions operating the geomagnetic observatories used in this study are acknowledged. The SEM EUV data were obtained from the SEM Web site (http://www.usc.edu) and the GOES 10 X-ray data were obtained from the NOAA FTP site (ftp://ftp.ngdc.noaa.gov). H. Liu is supported by the Japan Society for the Promotion of Science (JSPS) foundation for young scientists. The CHAMP mission is supported by the German Aerospace Center (DLR) in operation and by the Federal Ministry of Education and Research (BMBF) in data processing.

[24] Zuyin Pu thanks Takuya Tsugawa and Jann-Yenq Liu for their assistance in evaluating this paper.

References

Afraimovich, E. L., A. T. Altynsev, V. V. Grechnev, and L. A. Leonovich (2002), The response of the ionosphere to faint and bright solar flares as deduced from global GPS network data, *Ann. Geophys.*, *45*, 31–40.

Bruinsma, S., J. Forbes, R. Nerem, and X. Zhang (2006), Thermosphere density response to the 20–21 November 2003 solar and geomagnetic storm from CHAMP and GRACE accelerometer data, *J. Geophys. Res.*, *111*, A06303, doi:10.1029/2005JA011284.

Conde, M., et al. (2001), Assimilated observations of thermospheric winds, the aurora, and ionospheric currents over Alaska, *J. Geophys. Res.*, *106*, 10,493–10,508.

Davies, K. (1990), *Ionospheric Radio*, Peter Peregrinus, London.

Donnelly, R. F. (1969), Contribution of X-ray and EUV bursts of solar flares to sudden frequency deviations, *J. Geophys. Res.*, *74*, 255–259.

Donnelly, R. F. (1976), Empirical models of solar flare X ray and EUV emission for use in studying their E and F region effects, *J. Geophys. Res.*, *81*, 4745–4753.

Greenfield, S. M., and S. V. Venkateswaran (1968), The vertical structure of dynamo winds deduced from geomagnetic variations associated with solar flares, *Ann. Geophys.*, *24*, 665–672.

Kelley, M. C. (1989). *The Earth's Ionosphere*, Academic, New York.

Killeen, T. L., and R. Roble (1984), An analysis of the high-latitude thermospheric wind pattern calculated by a thermospheric general circulation model: 1. Momentum forcing, *J. Geophys. Res.*, *89*, 7509–7522.

Liu, H., and H. Lühr (2005), Strong disturbance of the upper thermospheric density due to magnetic storms: CHAMP observations, *J. Geophys. Res.*, *110*, A09S29, doi:10.1029/2004JA010908.

Liu, H., H. Lühr, V. Henize, and W. Köhler (2005), Global distribution of the thermospheric total mass density derived from CHAMP, *J. Geophys. Res.*, *110*, A04301, doi:10.1029/2004JA010741.

Liu, H., H. Lühr, and S. Watanabe (2007), Climatology of the equatorial mass density anomaly, *J. Geophys. Res.*, *112*, A05305, doi:10.1029/2006JA012199.

Liu, J. Y., C. S. Chiu, and C. H. Lin (1996), The solar flare radiation responsible for sudden frequency deviation and geomagnetic fluctuation, *J. Geophys. Res.*, *101*, 10,855–10,862.

Liu, J. Y., C. H. Lin, Y. I. Chen, Y. C. Lin, T. W. Fang, C. H. Chen, Y. C. Chen, and J. J. Hwang (2006), Solar flare signatures of the ionospheric GPS total electron content, *J. Geophys. Res.*, *111*, A05308, doi:10.1029/2005JA011306.

Manju, G., and K. S. Viswanathan (2005), Response of the equatorial electrojet to solar flare related X-ray flux enhancement, *Earth Planets Space*, *57*, 231–242.

Manoj, C., H. Lühr, S. Maus, and N. Nagarajan (2006), Evidence for short spatial correlation lengths of the noontime equatorial electrojet inferred from a comparison of satellite and ground magnetic data, *J. Geophys. Res.*, *111*, A11312, doi:10.1029/2006JA011855.

Mitra, A. P. (1974), *Ionospheric Effects of Solar Flares*, Reidel, D., Boston.

Ohshio, M. (1971), Negative sudden phase anomaly, *229*, *Nature*, 239–244.

Rastogi, R. G., B. M. Pathan, D. R. K. Rao, T. S. Sastry, and J. H. Sastri (1999), Solar flare effects on the geomagnetic elements during normal and counter electrojet periods, *Earth Planets Space*, *51*, 947–957.

Richmond, A. D. (1973), Equatorial electrojet. I. Development of a model including winds and instabilities, *J. Atmos. Terr. Phys.*, *35*, 1083–1103.

Richmond, A. D., and S. V. Venkateswaran (1971), Geomagnetic crochets and associated ionospheric current systems, *Radio Sci.*, *6*, 139–164.

Stonehocker, G. H. (1970), Advanced telecommunication forecasting technique in AGY, in *Ionospheric Forecasting, AGARD Conf. Proc.*, 29, 27–31.

Sutton, E. K., J. M. Forbes, R. S. Nerem, and T. N. Woods (2006), Neutral density response to the solar flares of October and November, 2003, *Geophys. Res. Lett.*, *33*, L22101, doi:10.1029/2006GL027737.

Thome, G. D., and L. S. Wagner (1971), Electron density enhancements in the E- and F-regions of the ionosphere during solar flares, *J. Geophys. Res.*, *76*, 6883–6895.

Tsugawa, T., T. Sadakane, J. Sato, Y. Otsuka, T. Ogawa, K. Shiokawa, and A. Saito (2006), Summer-winter hemispheric asymmetry of sudden increase in ionospheric total electron content induced by solar flares: A role of o/n_2 ratio, *J. Geophys. Res.*, *111*, A11316, doi:10.1029/2006JA011951.

Tsurutani, B. T., et al. (2005), The October 28, 2003 extreme EUV solar flare and resultant extreme ionospheric effects: comparison to other Halloween events and the Bastille Day event, *Geophys. Res. Lett.*, *32*, L03S09, doi:10.1029/2004GL021475.

Tsurutani, B. T., et al. (2006), Extreme solar EUV flares and ICMEs and resultant extreme ionospheric effects: Comparison of the Halloween 2003 and the Bastille Day events, *Radio Sci.*, *41*, RS5S07, doi:10.1029/2005RS003331.

Zhang, D. H., and Z. Xiao (2003), Study of ionospheric total electron content response to the great flare on 15 april 2001 using Internation GPS Service network for the whole sunlit hemisphere, *J. Geophys. Res.*, *108*(A8), 1330, doi:10.1029/2002JA009822.

Zhang, D. H., and Z. Xiao (2005), Study of ionospheric response to the 4B flare on 28 october 2003 using Internation GPS Service network data, *J. Geophys. Res.*, *110*, A03307, doi:10.1029/2004JA010738.

H. Liu and S. Watanabe, Earth and Planetary Science Division, Hokkaido University, Sapporo 060-0810, Japan. (huixin@gfz-potsdam.de)

H. Lühr and W. Köhler, GeoForschungZentrum Potsdam, D-14473 Potsdam, Germany.

C. Manoj, Magnetotellurics Division, National Geophysical Research Institute, Hyderabad 500 007, India.